

# Aerospace launch vehicle control: a gain scheduling approach

Benoît Clement<sup>a</sup>, Gilles Duc<sup>b,\*</sup>, Sophie Mauffrey<sup>c</sup>

<sup>a</sup> CNES, Direction des Lanceurs, Rond Point de l'Espace, 91023 Evry, Cedex, France

<sup>b</sup> Ecole Supérieure d'Electricité, Service Automatique, 3 rue Joliot Curie, F91192 Gif-sur-Yvette, Cedex, France

<sup>c</sup> EADS Space Transportation, BP 2, 78133 Les Mureaux, Cedex, France

Received 5 February 2003; accepted 20 December 2003

## Abstract

This paper presents a methodology for designing an aerospace launch vehicle autopilot. Linear controllers are first designed using a multi-objective method based on the Youla parameterization and the optimization under constraints described by linear matrix inequalities. These controllers are then interpolated in such a way that the stability of the closed-loop plant is guaranteed. Results obtained from a nonlinear simulator against wind disturbances and parameter uncertainties are then given.

© 2004 Elsevier Ltd. All rights reserved.

**Keywords:** Aerospace launch vehicle; Gain scheduling; Interpolation; Discrete-time systems; Multi-objective control; Linear matrix inequalities

## 1. Introduction

This paper presents a gain scheduling application for an aerospace launch vehicle; it concerns the atmospheric flight control which is a nonstationary step of the mission due to the evolution of the main physical parameters (mass, velocity, gravity, etc.). The launch vehicle control during the atmospheric flight has been investigated in the automatic control literature; during the last years, studies have been performed for instance by the CNES (French Space Agency) and EADS Launch Vehicles (Mauffrey & Schoeller, 1998; Clement, Duc, Mauffrey, & Biard, 2001; Voinot, Alazard, & Piquereau, 2001; Mauffrey, Meunier, Pignié, Biard, & Rongier, 2001).

The nonstationary characteristics during the atmospheric flight imposes to use a gain scheduling approach for such a plant which is modeled as a linear time-varying (LTV) system. The variations of the main parameters of the launcher model are known as functions of time, but subject to uncertainties. Furthermore, bending modes are to be taken into account. The methodology proposed in this paper is as follows. Different operating points are chosen along the launcher trajectory, which is known in advance. For each of them, a linear controller is designed: independent  $H_\infty$  norm constraints are considered to enforce the performance while guaranteeing robustness properties, using a multi-objective design method based on the Youla parameterization. The controllers so obtained are then interpolated with a particular attention on guaranteeing the stability. All steps of the design involve optimization under linear matrix inequalities (LMI) constraints.

The paper is organized as follows. Section 2 gives a presentation of the plant and the control objectives; Section 3 is dedicated to the multi-objective design, and Section 4 to the gain scheduling problem with a particular attention on the interpolation method. Then Section 5 shows the results obtained with a simulator which has been developed with the CNES (French Space Agency) and EADS Launch Vehicles: a wind disturbance and parameter uncertainties are simultaneously considered.

\*Corresponding author. Tel.: +33-1-69-85-13-88; fax: +33-1-69-85-12-34.

E-mail address: [gilles.duc@supelec.fr](mailto:gilles.duc@supelec.fr) (G. Duc).

**Remark 1.** For confidentiality reasons, the numerical values cannot be given in the paper. However, the constraints introduced by the specifications (see Section 2) will be plotted on the simulation results, where in addition all time and frequency units are identical for all plots.

## 2. Launch vehicle control

The automatic control of the launcher has the function of keeping the process stable around its center of gravity, following the guidance reference trajectory (Fig. 1).

This paper considers the design of the autopilot for the atmospheric flight phase. In order to simplify, the application is developed for the yaw axis only; its dynamics include a rigid mode, bending modes (sloshing modes are not considered), actuators and sensors. The problem is to design a discrete-time controller with the following objectives:

- *Frequency-domain specifications:*
  - Closed-loop stability with sufficient margins: decreasing and increasing gain margins ( $\Delta G_{\text{inf}}$  and  $\Delta G_{\text{sup}}$ ) have to stay higher than given specifications.
  - Control the destabilizing bending modes: the aim is to attenuate these modes under a gain limit ( $X_{dB} < 0$ ) except for the first one which can be controlled in phase with a sufficient delay margin (at least one sample period  $T_s$ ).
- *Time domain specifications:*
  - Limit the angle of attack  $i$  in case of wind disturbance (a typical wind profile will be given in Fig. 12).
  - Limit the angle of deflection  $\beta$  and its velocity  $\dot{\beta}$ .
  - The consumption  $C$  must be limited to  $C_{\text{max}}$  where

$$C = \sum_{k=T_{\text{init}}}^{T_{\text{end}}} |\beta(k+1) - \beta(k)|. \quad (1)$$

- *Robustness*
  - All these objectives have to be robust against uncertainties (which affect rigid and bending modes).

A simplified launcher scheme is given in Fig. 2 where the angle of attack between the launcher axis and the relative speed  $V_R$  is noted  $i$ , the attitude  $\psi$ , the angle of deflection  $\beta$  (control input) and the wind velocity  $W$  (disturbance). The

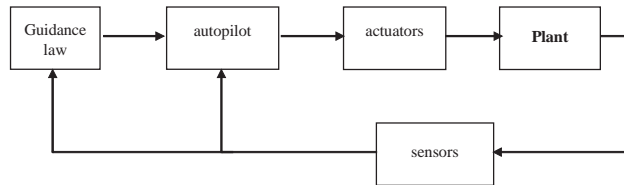


Fig. 1. Control loops.

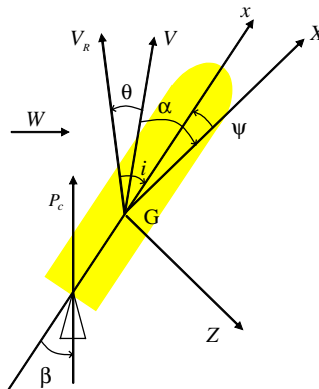


Fig. 2. Simplified launcher representation.

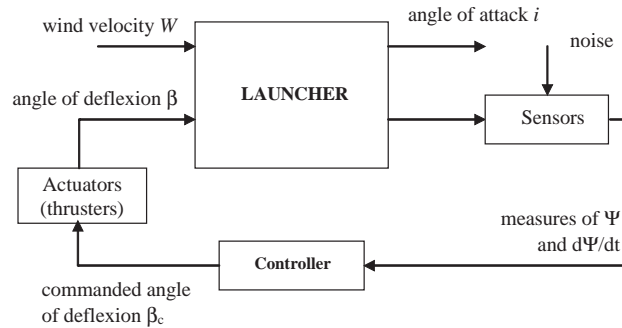


Fig. 3. Control structure.

sensors allow measuring the attitude and its velocity whereas the actuators allow controlling the angle of deflection for the thrusters.

The challenge of such a control issue is to minimize the angle of attack  $i$  which in addition cannot be measured. The closed-loop structure is given in Fig. 3.

The simplified model of the process is already LTV (only small angles are considered and saturations have to be avoided). The control design is performed along the guidance trajectory by considering several operating points: for each of them, a linear controller is performed to meet the design specifications using the multi-objective algorithm presented in Section 3, which is based on Youla parameterization and LMI optimization. This algorithm reduces the conservatism of previously existing methods.

Next, the obtained controllers are interpolated using the method presented in Section 4 for which stability is guaranteed: it is particularly adapted to the launcher problem because the evolution of the parameters is known as continuous functions of time.

**Remark 2.** One can ask about the signification of frequency-domain specifications for a time-varying plant: on one hand, although some physical parameters (mass, dynamic pressure, etc.) are rapidly changing, the parameters which define the dynamics (rigid modes, natural frequencies of the bending modes, etc.) are known to be slowly varying with respect to the closed-loop dynamics of the autopilot; on the other hand, such specifications are meaningful from an industrial point of view (so that they are widely used for European and American launchers).

### 3. Multi-objective control

Control design often involves tradeoffs among conflicting objectives. Most of the time the controller is required to satisfy simultaneously different performance and robustness objectives which are imposed on different channels of the closed-loop plant. Some discussion about multi-objective control first appeared for instance in Boyd and Barrat (1991); Dorato (1991); Khargonekar and Rotea (1991). In particular, design under  $H_2$  and  $H_\infty$  constraints has received many attentions. Tractable convex optimization formulations were derived in the literature but the first proposed methods were conservative: they used a single common Lyapunov function for each synthesis objective and a change of variable which simultaneously affects this Lyapunov function and the controller (Kaminer, Khargonekar, & Rotea, 1993; Scherer, Gahinet, & Chilali, 1997).

More recently, Youla parameterization has been proved to be useful to reduce this conservatism (Hindi, Hassidi, & Boyd, 1998; Scherer, 1999); following the way initiated by the later work, the method used in this paper was first proposed in (Clement & Duc, 2000): it uses an independent Lyapunov function for each objective, a change of variables on these functions but not on the controller, and an observer-based structure which allows to reduce the degree of the controller. The solution is obtained using LMI optimization that is now a computationally tractable framework. It is described in the following sections.

#### 3.1. Notations and performance specifications

All plants considered in Section 3 are LTI finite dimensional, and described by a discrete-time state-space realization (with sample frequency  $f_s = 1/T_s$ ). Closed-loop plants are represented by the standard diagram of Fig. 4, where vector

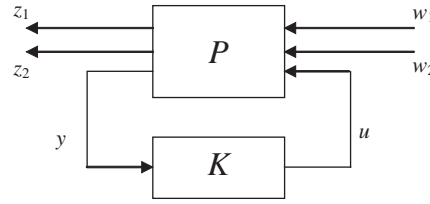


Fig. 4. Closed-loop representation.

$u$  denotes the control input, vector  $y$  the measured output, and channels from vector  $w_i$  (external input) to vector  $z_i$  (controlled output) are used to specify two different robustness or performance objectives.

State-space representations of the open-loop plant  $P$  and the controller  $K$  are noted as

$$P = \left( \begin{array}{c|ccc} A & B_1 & B_2 & B_u \\ \hline C_1 & D_{11} & D_{12} & D_{1u} \\ C_2 & D_{21} & D_{22} & D_{2u} \\ \hline C_y & D_{y1} & D_{y2} & D_{yu} \end{array} \right), \quad (2)$$

$$K = \left( \begin{array}{c|c} A_K & B_K \\ \hline C_K & D_K \end{array} \right). \quad (3)$$

Without loss of generality, it is assumed in the paper that  $D_{yu} = 0$ .

Interconnection of two plants will be noted by the Redheffer star product. As a particular case, the closed-loop plant of Fig. 4 is noted  $P \star K$ .

The objectives under consideration in this paper are to control the  $H_\infty$  norm of each transfer from  $w_i$  to  $z_i$ ;  $H_\infty$  norm constraints are useful to enforce robustness and to express frequency-domain specifications. They are considered below with an LMI formulation. Other objectives like  $H_2$  norm or time domain constraints can also be translated into LMI formulations and can also be used in the proposed multi-objective control approach (Clement & Duc, 2000).

The goal of the multi-objective synthesis is the Pareto optimal controller which is well representative of the tradeoff between conflicting objectives. It consists in minimizing a linear combination of different objectives (here the  $H_\infty$  norm of each transfer).

It is well known that this problem is hard and nonconvex (Boyd & Barrat, 1991). To perform a synthesis via convex optimization, it is necessary to transform the initial problem. A combination of the different tools presented in this section leads to the synthesis algorithm given in Section 3.6. The three tools are the following:

- the Youla parameterization gives specific properties to the system,
- the observer-based structure allows to reduce the degree of the controller,
- the optimization of the Youla parameter is expressed as an LMI problem.

Besides, most of the LMI-based multi-objective methods use a common Lyapunov function for every objectives to make the synthesis tractable. On the contrary, the approach described below allows to choose different functions for each objective without losing convexity (see Section 3.4); this is a crucial point to reduce the conservatism of the design.

### 3.2. Youla parameterization

Consider the plant model (2). Suppose there exists matrices  $K_c, K_f$  of appropriate dimensions such that  $A - BK_c$  and  $A - K_f C$  are stable. Then the set of all stabilizing controllers for (2) can be parameterized (Maciejowski, 1989) as  $K = JQ$  (see Fig. 5), where  $J$  is described by

$$J = \left( \begin{array}{c|cc} A - B_u K_c - K_f C_y & K_f & B_u \\ \hline -K_c & 0 & I \\ \hline -C_y & I & 0 \end{array} \right) \quad (4)$$

and  $Q$  is a stable transfer function. Obviously, such matrices  $K_c, K_f$  can be obtained using standard state-feedback and observer design techniques. In a multi-objective control strategy however, it can be more efficient to start with an initial

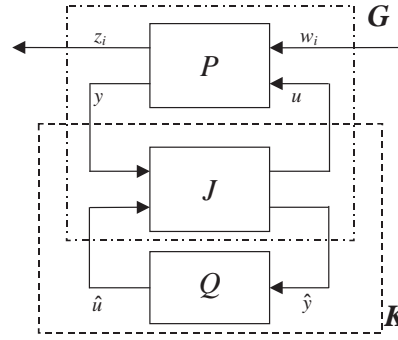


Fig. 5. Closed-loop structure with Youla parameterization.

controller which partly satisfies the control objectives. The next subsection explains how to transform any controller in the observer-based structure required for the Youla parameterization.

### 3.3. Observer-based structure for arbitrary compensators

This question has been investigated for instance in Alazard and Apkarian (1999), which in addition, contains various references on this subject. Only the main results are summarized here.

Consider a plant  $P$  of degree  $n$  described by (2) and a controller  $K$  of degree  $n_c \geq n$  described by (3). Under weak assumptions, there exist matrices  $K_c$ ,  $K_f$  and a Youla parameter  $Q$  of degree  $n_c - n$  such that  $K = J * Q$ , with  $J$  described by (4).

For simplicity, only the parameterization of a controller  $K$  with the same order as the plant  $P$  is presented in the following. In that case,  $Q$  is a gain matrix. The equivalence between  $K$  given by (3) and  $J * Q$  is obtained by looking for a regular matrix  $T$  such that (Alazard & Apkarian, 1999)

$$\begin{aligned} T^{-1}A_K T &= A - B_u K_c - K_f C_y - B_u Q C_y, \\ T^{-1}B_K &= K_f + B_u Q, \\ C_K T &= -K_c - Q C_y, \\ D_K &= Q. \end{aligned} \quad (5)$$

By elementary manipulations, (5) leads to a generalized Riccati equation in  $T$ :

$$A_K T - T(A + B_u D_K C_y) - T B_u C_K T + B_K C_y = 0 \quad (6)$$

from which  $K_c$ ,  $K_f$  are immediately obtained using again (5).

**Remark 3.** Eq. (6) can be solved using standard invariant subspace techniques. There are a combinatory number of solutions according to the choice of the partition of the eigenvalues of the corresponding Hamiltonian matrix (which is in fact the closed-loop state matrix). Some rules are proposed in Alazard and Apkarian (1999); Fowell and Bender (1985) to help the choice. Reduced and augmented order controller cases are also considered in Alazard and Apkarian (1999).

### 3.4. Convex optimization of a static Youla parameter

A fundamental property of the Youla parameterization (Maciejowski, 1989) is the following: for the system  $G = P * J$  (Fig. 5), the transfer between  $\hat{u}$  and  $\hat{y}$  is identically zero, or equivalently the nonobservable and noncontrollable subspaces of  $G$  are supplementary. Consequently, there exists a basis such that the system  $G$  admits the following state-space description:

$$G = \left( \begin{array}{cc|cc|c} A_1 & A_3 & B_{11} & B_{21} & \hat{B}_u \\ 0 & A_2 & B_{12} & B_{22} & 0 \\ \hline C_{11} & C_{12} & \hat{D}_{11} & \hat{D}_{12} & \hat{D}_{1u} \\ C_{21} & C_{22} & \hat{D}_{21} & \hat{D}_{22} & \hat{D}_{2u} \\ \hline 0 & \hat{C}_y & \hat{D}_{y1} & \hat{D}_{y2} & 0 \end{array} \right). \quad (7)$$

The multi-objective control problem is now to find an (static) output feedback  $Q$  for the system  $G$ . The following theorem allows to consider simultaneously different  $H_\infty$  objectives.

**Theorem 1** (Clement & Duc, 2001). *The closed-loop transfer from  $w_i$  to  $z_i$  has a  $H_\infty$  norm less than  $\gamma_i$  if and only if there exist real matrices  $R_i = R_i^T > 0$ ,  $S_i$ ,  $T_i = T_i^T > 0$  and  $Q$  such that*

$$\left( \begin{array}{cc|cc|cc|c} -R_i & 0 & A_1 R_i & A_1 S_i - S_i A_2 + A_3 + \hat{B}_u Q \hat{C}_y & B_{11} + \hat{B}_u Q \hat{D}_{y1} - S_i B_{12} & 0 & \\ 0 & -T_i & 0 & T_i A_2 & T_i B_{12} & 0 & \\ \hline * & * & -R_i & 0 & 0 & R_i^T C_{11}^T & \\ * & * & 0 & -T_i & 0 & C_{12}^T + C_y^T Q^T \hat{D}_{1u}^T + S_i^T C_{11}^T & \\ \hline * & * & * & * & -\gamma_i I & \hat{D}_{11}^T + \hat{D}_{y1}^T Q^T \hat{D}_{1u}^T & \\ * & * & * & * & * & -\gamma_i I & \end{array} \right) < 0. \quad (8)$$

Considering now both channels of  $G$ , one obtains two LMIs of the form (8) with the same Youla parameter  $Q$ , two  $H_\infty$  levels  $\gamma_1, \gamma_2$  and different matrices  $R_1, S_1, T_1, R_2, S_2, T_2$ . So the multi-objective problem depends affinely on these variables and  $Q$ ; it is therefore a convex problem which can be solved using any software dedicated to optimization under LMI constraints.

### 3.5. Convex optimization of a dynamic Youla parameter

The previous results can be directly extended to the design of a dynamic Youla parameter. Suppose a parameter of order  $r$  is looked for. A natural way is to define an augmented system by choosing as measurement not only  $\hat{y}(k)$  but  $(\hat{y}(k)^T \cdots \hat{y}(k-r)^T)^T$ . The previous results still hold for the corresponding augmented system (Fig. 6).

### 3.6. Algorithm

The previous results yield to the following algorithm for multi-objective control based on the Youla parameterization:

- (i) *Initial synthesis*: design an initial controller using conventional techniques (such as LQG methods,  $H_2$  or  $H_\infty$  optimization, or multi-objective control with a common matrix  $X$ ).
- (ii) *Observer-based structure parameterization*: solve Eqs. (5) and (6) and obtain the Youla parameterization with  $J$  described by (4).
- (iii) *Convex optimization*: choose the order of the Youla parameter  $Q$  and solve the multi-objective control problem using the LMIs of Section 3.4; the final controller is obtained as  $K = J * Q$ .

**Remark 4.** From a practical point of view, it can be inferred that the quality of the results partly depends on the quality of the initial controller. Therefore, a conventional  $H_\infty$  design could be an adequate choice for step (i).

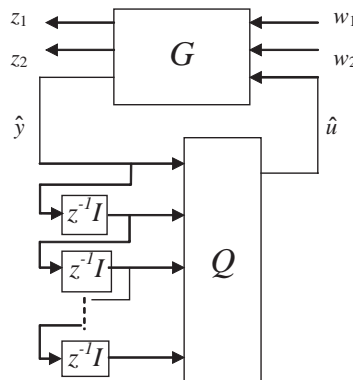


Fig. 6. Design of a dynamic parameter using an augmented system.

#### 4. Gain scheduling

The gain scheduling approach is a very classical nonlinear control technique which first appears in industrial fields (in particular for aeronautic and military applications) and have been theoretically investigated since the 1990s (Rugh, 1991). Roughly speaking, it can be described as a six-step procedure:

1. get a linear parameter-varying model,
2. choose the scheduling parameters,
3. choose a family of operating points,
4. compute controllers for each point with linear design methods,
5. interpolate these controllers using some appropriate method,
6. check the performance specifications.

Though differing technical avenues are available at each step, the scheme stays the same. Among papers that have investigated gain scheduling (Rugh & Shamma, 2000), very little focus in the interpolation problem, which is a fundamental step in the synthesis of a scheduled control law. In the literature, a number of ad hoc approaches have been presented (Reichert, 1992; Nichols, Reichert, & Rugh, 1993; Hyde & Glover, 1993; Buschek, 1997) but the specifications are checked a posteriori.

More recently, interpolation of continuous-time state-space controllers while preserving stability has been considered in Stilwell and Rugh (2000). The same authors consider also the case of observer-based state-feedback controllers (Stilwell & Rugh, 1999): solving LMI conditions for different operating points allow deriving varying state-feedback and observer gains while guaranteeing exponential stability. This later work was the starting point of the approach developed below, which considers the problem in discrete time.

##### 4.1. Notations and definitions

The considered model is the same as in Section 3, except that all matrices are now time-varying:

$$\begin{aligned} x(k+1) &= A(k)x(k) + B_w(k)w(k) + B_u(k)u(k), \\ z(k) &= C_z(k)x(k) + D_{zw}(k)w(k) + D_{zu}(k)u(k), \\ y(k) &= C_y(k)x(k) + D_{yw}(k)w(k). \end{aligned} \quad (9)$$

Theoretical results about gain scheduling (Shamma, 1988; Shamma & Athans, 1990; Fromion, Monaco, & Normant-Cyrot, 1996) are often hard to be used in a practical way because of the generality of the field of gain scheduling. The choice of a closer class of systems seems to be a way to particularize some general results and to justify rigorously practical applications. According to the space launcher problem, the results presented in this paper consider an LTV system following a known trajectory. Indeed, all launcher parameters are known as functions of time.

The proposed method is presented in the next section jointly with a sufficient condition to preserve stability with the LTV plant. For ease of understanding, the paper mainly focuses on the state-feedback case; the case of a dynamic output feedback controller is then considered.

##### 4.2. Interpolation of state-feedback controllers

For brevity, the state-feedback case is considered with only two models corresponding to different instants  $k_1$  and  $k_2$ . Let two state-feedback gains  $K_1$  and  $K_2$  such that  $A(k) + B_u(k)K_1$  and  $A(k) + B_u(k)K_2$  are stable for each frozen value of  $k$  in some neighborhoods  $[a, c]$  and  $[b, d]$  of  $k_1$  and  $k_2$ , respectively (Fig. 7). Assume that  $b < c$ , such that  $K_1$  and  $K_2$  are simultaneously stabilizing for each frozen  $k$  in  $[b, c]$ .

**Theorem 2 (Clement & Duc, 2001).** *If there exist two symmetric positive definite matrices  $X_1$  and  $X_2$  and a strictly positive  $\gamma$  such that the following relations hold:*

$$(i) \quad \forall k = a, \dots, c: \quad \begin{pmatrix} -X_1 & (A(k) + B_u(k)K_1)X_1 \\ X_1(A(k) + B_u(k)K_1)^T & -X_1 \end{pmatrix} < -\gamma I, \quad (10a)$$



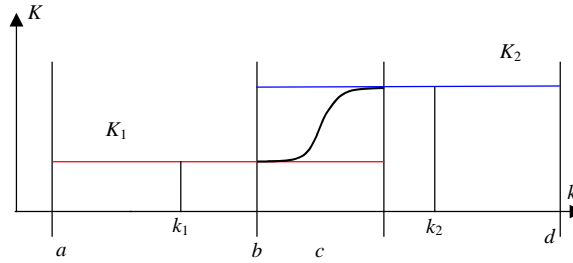


Fig. 7. State-feedback gain evolution.

$$(ii) \quad \forall k = b, \dots, d : \begin{pmatrix} -X_2 & (A(k) + B_u(k)K_2)X_2 \\ X_2(A(k) + B_u(k)K_2)^T & -X_2 \end{pmatrix} < -\gamma I, \quad (10b)$$

$$(iii) \quad X_1 - X_2 < (c - b)\gamma I \quad (10c)$$

then the scheduled state-feedback gain

$$K(k) = \begin{cases} K_1 & \text{if } a \leq k \leq b, \\ \left( \frac{c-k}{c-b} K_1 X_1 + \frac{k-b}{c-b} K_2 X_2 \right) \left( \frac{c-k}{c-b} X_1 + \frac{k-b}{c-b} X_2 \right)^{-1} & \text{if } b \leq k \leq c, \\ K_2 & \text{if } c \leq k \leq d \end{cases} \quad (11)$$

is such that the closed-loop LTV system is exponentially stable.

#### Remark 5.

- The interpolation is performed only on the discrete-time interval  $[b \ c]$  where both controllers are stabilizing.
- The constraints are LMIs in  $X_1, X_2$  which allow to ensure stability with convex optimization.
- Condition (10.c) is original because no norm is considered. It is made possible by the knowledge of the trajectory. This is a difference with the continuous-time results of Stilwell & Rugh (1999), where the norm of  $X_1 - X_2$  limit the allowable rate of the scheduling parameter variations.

Note that the interpolation turns into linear interpolation as a particular case. Indeed, if there is a solution such that  $X_1 = X_2 = X$ , the gain becomes a linear interpolation:

$$K(k) = \begin{cases} K_1 & \text{if } a \leq k \leq b, \\ \frac{c-k}{c-b} K_1 + \frac{k-b}{c-b} K_2 & \text{if } b \leq k \leq c, \\ K_2 & \text{if } c \leq k \leq d. \end{cases} \quad (12)$$

This is possible when the two consecutive gains and frozen time plants are rather closed. In this case there exists a common Lyapunov function  $X_1 = X_2$  such that inequalities (10a) and (10b) hold while (10c) is obviously satisfied.

#### 4.3. Interpolation of observer gains

The interpolation of a full order observer is the dual problem. Assume that  $L_1$  and  $L_2$  are two observer gains such that  $A(k) + L_1 C_2(k)$  and  $A(k) + L_2 C_2(k)$  are stable for each frozen value of  $k$  in some neighborhoods  $[a \ c]$  and  $[b \ d]$  of  $k_1$  and  $k_2$ , respectively, with  $b < c$ . If there exist two symmetric positive definite matrices  $X_1$  and  $X_2$  and a strictly positive  $\gamma$  such that

$$(i) \quad \forall k = a, \dots, c : \begin{pmatrix} -X_1 & (A(k) + L_1 C_y(k))^T X_1 \\ X_1(A(k) + L_1 C_y(k)) & -X_1 \end{pmatrix} < -\gamma I, \quad (13a)$$



$$(ii) \quad \forall k = b, \dots, d : \begin{pmatrix} -X_2 & (A(k) + L_2 C_y(k))^T X_2 \\ X_2(A(k) + L_2 C_y(k)) & -X_2 \end{pmatrix} < -\gamma I, \quad (13b)$$

$$(iii) \quad X_1 - X_2 < (c - b)\gamma I \quad (13c)$$

then the scheduled observer gain

$$L(k) = \begin{cases} L_1 & \text{if } a \leq k \leq b, \\ \left( \frac{c-k}{c-b} X_1 + \frac{k-b}{c-b} X_2 \right)^{-1} \left( \frac{c-k}{c-b} X_1 L_1 + \frac{k-b}{c-b} X_2 L_2 \right) & \text{if } b \leq k \leq c, \\ L_2 & \text{if } c \leq k \leq d \end{cases} \quad (14)$$

is such that the LTV observer is exponentially stable.

#### 4.4. Interpolation of observer-based controllers

These results allow directly the interpolation of an observer-based controller: according to the separation theorem, the closed-loop dynamics is simply the concatenation of state-feedback and observer dynamics. The state-feedback gain and the observer gain can thus be interpolated according to Sections 4.2 and 4.3, while the exponential stability is guaranteed.

#### 4.5. Interpolation of nonstructured controllers

As explained in Section 3.3, almost any controller of order  $n_c \geq n$  can be interpreted as an observed state-feedback structure connected with a dynamic Youla parameter. Then the interpolation can be extended to controllers designed with various methods by interpolating the state-feedback gains, the observer gains and the Youla parameter of the equivalent observer/state-feedback structure. Note however that stability can no longer be guaranteed except for one of the following cases (Clement, 2001):

- the Youla parameter is time-invariant along the trajectory (so that it has not to be interpolated),
- linear interpolations are performed for the state-feedback gains, the observer gains and the Youla parameter.

### 5. Aerospace launcher control

#### 5.1. Gain scheduling procedure

This section describes the six steps of the gain scheduling procedure given in Section 4.

*Steps 1 and 2* are given by the choice of the model. Indeed, the LTV structure of the model is known as a table giving all parameters of the launcher at each instant  $k$ .

*Step 3*: the set of operating points is chosen in order to take into account the critical points; 10 points are chosen with constant intervals:

$$k_i = T_{init} + i \frac{T_{end} - T_{init}}{10}. \quad (15)$$

Note that some intervals could be split if the procedure failed. This case could occur if the parametric variations were high.

*Step 4*: 10 controllers are performed according to the multi-objective design presented in Section 3: this step is detailed in the following.

The model used for the design includes the rigid mode with the actuator and sensors dynamics; the bending modes are not included in the model, and will be considered as dynamic uncertainties. The synthesis scheme is given in Fig. 8. It is the same for all operating points to ensure that the interpolation can be easily performed. The three steps of Algorithm 3.6 are performed as follows:

- The initial synthesis is performed by considering only the  $H_\infty$  norm between  $w_1$  and  $i$  (i.e. the effect of the wind disturbance on the incidence), with a frequency-dependent weighting function  $W_1$ : it is a

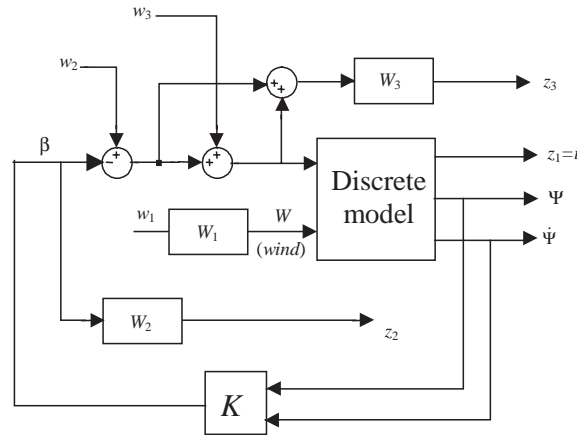


Fig. 8. Synthesis scheme.

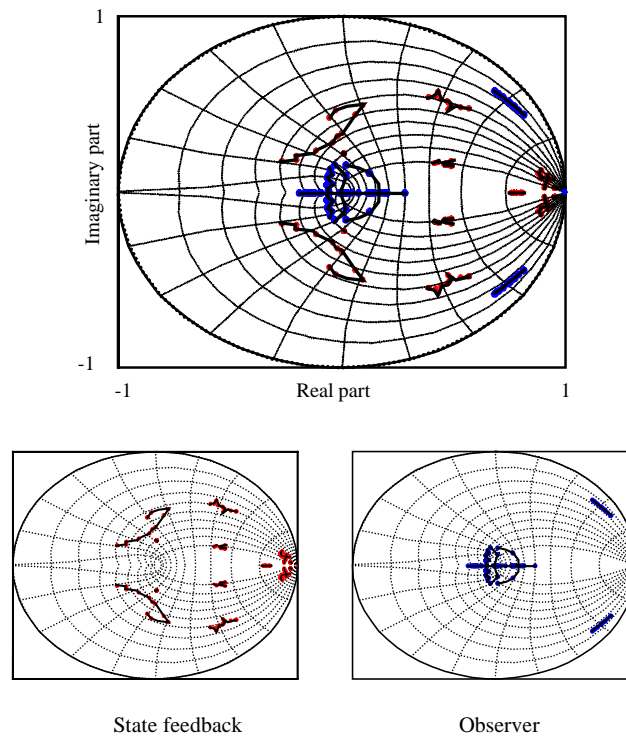
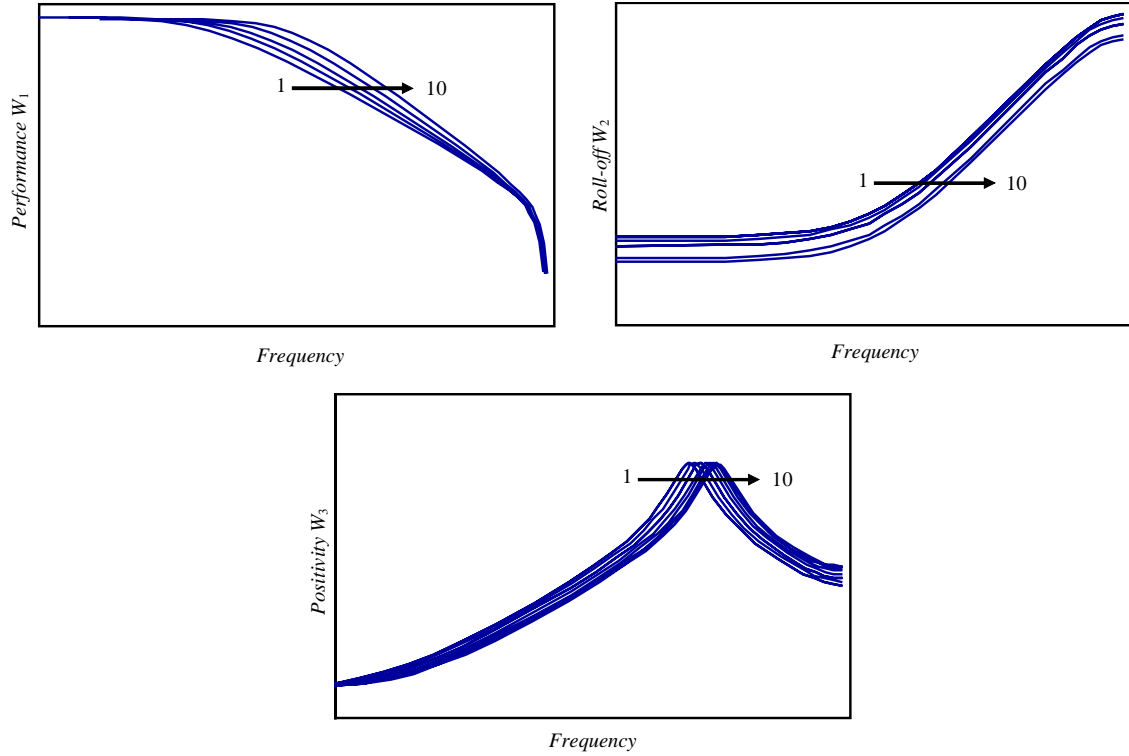


Fig. 9. Closed-loop eigenvalues map and affection.

second-order low-pass filter, to emphasize the fact that wind disturbances are generally slower as the launcher dynamics.

- (ii) The transformation of this first controller into an observer-based controller interconnected with a Youla parameter requires to choose which dynamics are from the observer and which ones are from the state feedback. This choice is done to insure the continuity of the closed-loop dynamics partition from one operating point to another: this is shown in Fig. 9, where the first plot gives the closed-loop eigenvalues for all operating points, whereas the small plots indicate those affected to the state feedback and the observer dynamics, respectively. Note that the evolutions of the controller parameters stay smooth as indicated by the eigenvalues evolution.
- (iii) a multi-objective synthesis is then performed by looking for a Youla parameter of order 2, and considering two independent  $H_\infty$  constraints:

$$\left\| \begin{pmatrix} W_1 T_{W \rightarrow i} & T_{w_2 \rightarrow i} \\ W_2 W_1 T_{W \rightarrow \beta} & W_2 T_{w_2 \rightarrow \beta} \end{pmatrix} \right\|_\infty < \gamma_1, \quad (16a)$$

Fig. 10. Gains of the filters used for  $H$  multi-objective syntheses.

$$\|W_3(S - T)\|_\infty < \gamma_2, \quad (16b)$$

where  $S = (I - L)^{-1}$ ,  $T = -LS$  and  $L$  are respectively the sensitivity function, the complementary sensitivity function and the open-loop transfer function (assuming positive feedback). By choosing  $W_3$  as a narrow second-order band-pass filter centered on the frequency of the first bending mode, (16b) is a positivity criterion which allows controlling the phase of the open-loop transfer function at all frequencies where the gain of  $W_3$  is large; in fact, it is easy to establish that

$$|S(e^{j\omega T_s}) - T(e^{j\omega T_s})| < 1 - \frac{\pi}{2} < \arg(-L(e^{j\omega T_s})) < \frac{\pi}{2} \quad (17)$$

$W_2$  is a roll off filter (i.e. a high-pass filter) of order 3, which is used to attenuate the open-loop gain at frequencies higher than the first mode, thus producing attenuation of the other modes.

These filters are to be tuned according to the evolution of the parameters; it has been noted that considering two independent objectives makes the tuning easier, whereas the  $H_\infty$  levels  $\gamma_1$  and  $\gamma_2$  are guaranteed to be smaller than the optimal  $H_\infty$  norm which would be obtained by considering simultaneously all transfers appearing in Fig. 8.

Fig. 10 shows the filter gains with respect to the 10 operating points.<sup>1</sup> The controller so obtained is of order 15 for each point.

*Step 5:* interpolations of the controllers have been performed according to the results of Section 4, by looking for a linear interpolation while preserving stability. For each interval, according to the notations in Theorem 2, the instants are chosen as  $a = b = k_i$  and  $c = d = k_{i+1}$  (which means that the interpolation is performed all along the trajectory). Then the state-feedback and observer gains are determined by looking for a common matrix  $X_i$  for each pair  $(k_i, k_{i+1})$ ; for instance, the following LMI problems are solved for the state-feedback gain:

$$\begin{pmatrix} -X_i & (A(k_i) + B_u(k_i)K_i)X_i \\ X_i(A(k_i) + B_u(k_i)K_i)^T & -X_i \end{pmatrix} < -\gamma I, \quad (18a)$$

<sup>1</sup> The frequency units are the same for the three plots.

$$\begin{pmatrix} -X_i & (A(k_{i+1}) + B_u(k_{i+1})K_{i+1})X_i \\ X_i(A(k_{i+1}) + B_u(k_{i+1})K_{i+1})^T & -X_i \end{pmatrix} < -\gamma I \quad (18b)$$

the existence of  $X_i$  allowing linear interpolation between  $K_i$  and  $K_{i+1}$  while guaranteeing stability. This is possible because it is known that the parameters are slowly varying. The same scheme holds for the observer gain, while the Youla parameter is also linearly interpolated. As explained in Section 4.5, exponential stability along the whole trajectory is therefore guaranteed.

Step 6 is useless for stability because it is guaranteed a priori. But the performances have to be checked; this is done in the next section with graphical interpretations.

## 5.2. Results

The efficiency of the method is now evaluated by considering the closed-loop plant with five bending modes; the obtained controller is applied to different models: they correspond to uncertainties on the rigid and bending modes parameters which have been recognized as worse case configurations.

The frequency open loop responses of the frozen systems with the bending modes are first considered in a Black–Nichols chart for the 10 operating points (Fig. 11). The + indicates the decreasing and increasing gain margin specifications, and the dashed line corresponds to the attenuation required for the bending modes up to the second one. It can be seen that the frequency-domain specifications are almost satisfied, even in the case of parameter dispersions.

Time responses of the closed-loop plant are then considered with respect to a typical worst case wind profile (Fig. 12) together with sensor noises. The specifications are represented by dark areas, whereas the time units are identical for all plots: the angle of attack  $i$  specification is almost satisfied for all cases (Fig. 13), the deflection angle  $\beta$  is far from the

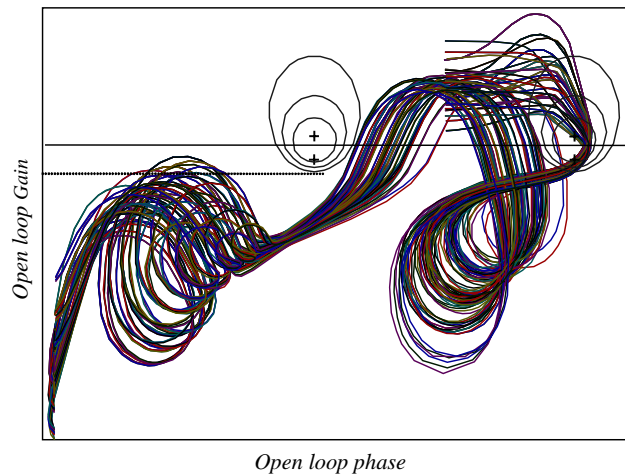


Fig. 11. Nichols chart for every operating point.

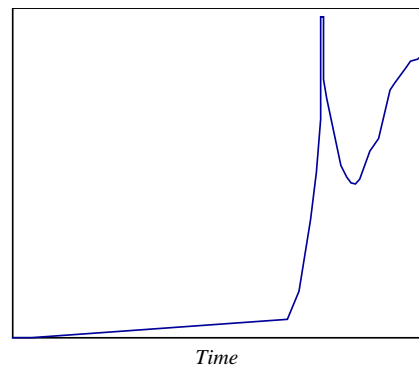
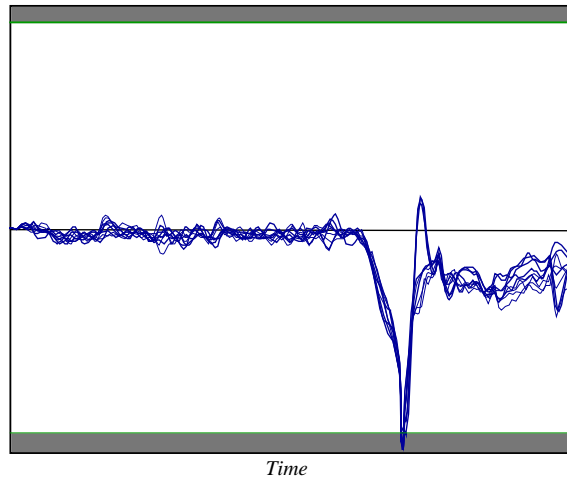
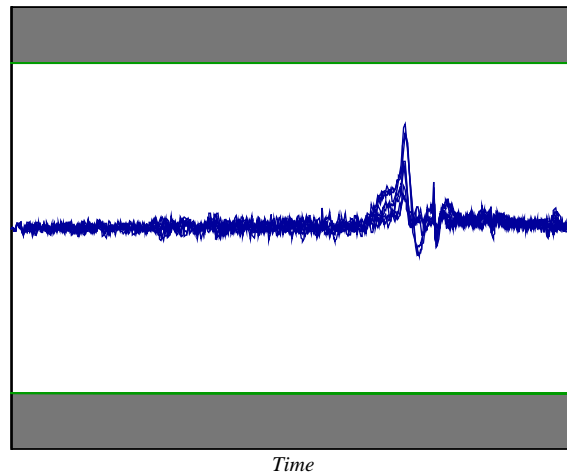
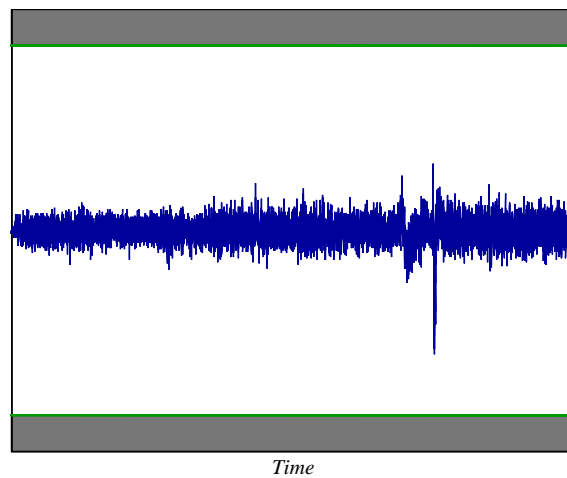


Fig. 12. Wind velocity profile.

Fig. 13. Angle of attack  $i$ .Fig. 14. Angle of deflection  $\beta$  (control).Fig. 15. Angle of deflection velocity  $\dot{\beta}$ .

saturations (Fig. 14), and it is the same for the velocity of the deflection angle  $d\beta/dt$  (Fig. 15). The attitude signal is given to underline the stability of the launcher (Fig. 16). The consumption constraint is clearly satisfied as shown in Fig. 17.

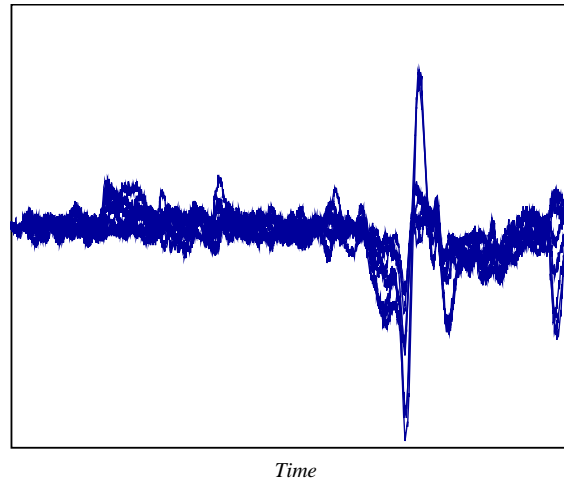
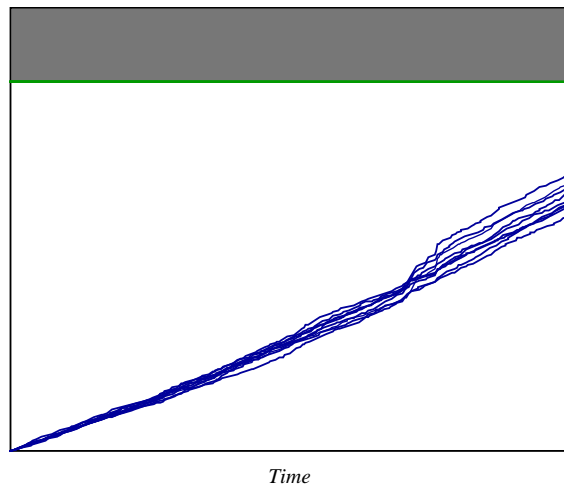
Fig. 16. Attitude  $\psi$ .

Fig. 17. Consumption.

## 6. Conclusion

The design of an autopilot for controlling the atmospheric flight of an aerospace launch vehicle has been considered. The plant model being linear time-varying, several controllers have first been designed by using a multi-objective method which allows considering independent  $H$  norms constraints, and thus independent performance and robustness objectives; it is based on the Youla parameterization and involves LMI optimization. These controllers are then linearly interpolated along the guidance trajectory, the interpolation method guaranteeing the closed-loop stability using again LMI optimization. When implementing this control law on a simulator, efficient results are obtained against a typical wind disturbance, despite parameter uncertainties. All the methods used in the paper are based on investigations about multi-objective design and gain scheduling which are largely discussed in the thesis (Clement, 2001).

## References

- Alazard, D., & Apkarian, P. (1999). Exact observer-based structures for arbitrary compensators. *International Journal of Robust & Non Linear Control*, 9, 101–118.
- Boyd, S., & Barrat, C. (1991). *Linear controller design: Limits of performance*. Englewood Cliffs, NJ: Prentice-Hall.
- Buschek, H. (1997). Robust autopilot design for future missile systems, *AIAA Guidance, navigation and control conference*, New Orleans.
- Clement, B. (2001). *Synthèse multiobjectifs et séquençement de gains: application au pilotage d'un lanceur spatial*. Ph. D. Thesis, Supélec and Université Paris XI.

- Clement, B., & Duc, G. (2000). Multiobjective control via Youla parameterization and LMI optimization: application to a flexible arm. *Third IFAC symposium on robust control design*, Prague.
- Clement, B., & Duc, G. (2001). An interpolation method for gain scheduling. *34th IEEE conference on decision and control*, Orlando.
- Clement, B., Duc, G., Mauffrey, S., & Biard, A. (2001). Gain scheduling for an aerospace launcher with bending modes. *15th IFAC symposium on automatic control in aerospace*, Bologna.
- Dorato, P. (1991). A survey of multiobjective design techniques. *Control of uncertain dynamical systems* (pp. 249–261). Boca Raton, FL: CRC Press.
- Fowell, D. J., & Bender, R. A. (1985). Computing the estimator-controller form of a compensator. *International Journal of Control*, 41, 1565–1575.
- Fromion, V., Monaco, S., & Normant-Cyrot, D. (1996). Robustness and stability of LPV plants through frozen system analysis. *International Journal Robust and Non Linear Control*, 6, 235–248.
- Hindi, H., Hassidi, B., & Boyd, S. (1998). Multiobjective  $H_2/H_\infty$ -optimal control via finite dimensional  $Q$ -parametrization and LMI. *American control conference*, Philadelphia (pp. 3244–3248).
- Hyde, A. R., & Glover, K. (1993). The application of scheduled  $H_\infty$  controllers to a VSTOL aircraft. *IEEE Transactions on Automatic Control*, 38, 1023–1039.
- Kaminer, I., Khargonekar, P. P., & Rotea, M. A. (1993). Mixed  $H_2/H_\infty$  control of discrete time systems via convex optimization. *Automatica*, 29, 27–70.
- Khargonekar, P. P., & Rotea, M. A. (1991). Mixed  $H_2/H_\infty$  control: a convex optimization approach. *IEEE Transactions on Automatic Control*, 36, 824–837.
- Maciejowski, J. (1989). *Multivariable feedback design*. Reading, MA: Addison-Wesley.
- Mauffrey, S., Meunier, P., Pignié, G., Biard, A., & Rongier, I. (2001).  $H_\infty$  control for the ARIANE 5 PLUS launcher. *52nd international astronautic congress*, Toulouse.
- Mauffrey, S., & Schoeller, M. (1998). Non-stationary  $H_\infty$  control for launcher with bending modes. *14th IFAC symposium on automatic control in aerospace*, Seoul.
- Nichols, R. A., Reichert, R. T., & Rugh, W. J. (1993). Gain scheduling for H-infinity controllers: A flight example. *IEEE Transactions on Control Systems Technologies*, 1, 69–79.
- Reichert, R. (1992). Dynamic scheduling of modern robust control autopilot designs for missiles. *IEEE Control Systems Magazines*, 12, 35–42.
- Rugh, W. J. (1991). Analytical framework for gain scheduling. *IEEE Control System Magazine*, 12, 79–84.
- Rugh, W. J., & Shamma, J. S. (2000). Research on gain scheduling. *Automatica*, 36, 1401–1425.
- Scherer, C. W. (1999). From mixed to multiobjective control. *IEEE conference on decision and control*, Phoenix.
- Scherer, C. W., Gahinet, P., & Chilali, M. (1997). Multi-objective output feedback control via LMI optimization. *IEEE Transactions on Automatic Control*, 42, 896–911.
- Shamma, S. (1988). *Analysis and design of gain scheduled control system*. Ph. D. thesis, The Massachusetts Institute of Technology.
- Shamma, J. S., & Athans, M. (1990). Analysis of gain scheduled control for nonlinear plants. *IEEE Transactions on Automatic Control*, 35, 898–907.
- Stilwell, D. J., & Rugh, W. J. (1999). Interpolation of observer state feedback controllers for gain scheduling. *IEEE Transactions on Automatic Control*, 44, 1225–1229.
- Stilwell, D. J., & Rugh, W. J. (2000). Stability preserving interpolation methods for the synthesis of gain-scheduled controllers. *Automatica*, 36, 665–671.
- Voinot, O., Alazard, D., & Piquereau, A. (2001). A robust multiobjective synthesis applied to launcher attitude control. *15th IFAC symposium on automatic control in aerospace*, Bologna.